

# Highly Efficient Hydroformylation of 1-Hexene over an *ortho*-Metallated Rhodium(I) Complex Anchored on a 2D-Hexagonal Mesoporous Material

Mahasweta Nandi,<sup>[a,b]</sup> Paramita Mondal,<sup>[c]</sup> Manirul Islam,<sup>[c]</sup> and Asim Bhaumik<sup>\*[a]</sup>

**Keywords:** Functionalisation / Heterogeneous catalysis / Hydroformylation / Mesoporous silica / Rhodium

The hydroformylation reaction is an important class of reaction as it enhances the carbon chain length of an olefin molecule. Rh<sup>I</sup> complexes are conventionally used as the catalyst for this reaction although they possess severe drawbacks with respect to separation and recycling. A phenyl-functionalised 2D-hexagonal mesoporous silica material has been synthesised by a surfactant templating pathway. The phenyl group of this mesoporous material was functionalised through nitration, followed by its reduction to the amine derivative. The amine group was further subjected to Schiff-

base condensation, and the Rh<sup>I</sup> complex was then heterogenised over its surface to yield the *ortho*-metallated complex anchored on the mesoporous silica matrix. The materials have been characterised by using powder X-ray diffraction, transmission electron microscopy and nitrogen adsorption/desorption studies. The Rh<sup>I</sup>-loaded mesoporous material acts as a very efficient catalyst for the hydroformylation reaction of 1-hexene and exhibits high selectivity towards the formation of *n*-heptanal at 343 K in the presence of H<sub>2</sub>/CO at 50 bar pressure.

## Introduction

Coordination compounds with the ability to catalyze the substrate to form the desired product with high selectivity by green synthetic routes have been drawing the attention of researchers over the last few decades.<sup>[1]</sup> Homogeneous catalysts based on transition metals are capable to act efficiently under mild conditions, and their selectivity can be tuned by varying the ligands attached to the metal centre.<sup>[2]</sup> The major problem associated with the use of homogeneous catalysts, however, is the separation of product(s) from the substrate and catalyst as all the components of the reaction mixture exist in a single phase. Isolation of the catalyst from the solution is often a challenging task. The loss of the catalyst in homogeneous catalysis is not acceptable for economical, environmental and toxicological reasons. Poor reusability of such catalysts is another concern. Catalysts with minimum effort to separate from the reaction mixture and high recycling efficiency are required for industrial utilisation. Binding the catalysts to organic or inorganic solid supports is a widely used procedure for heterogenising the homogeneous catalysts. The attachment of homogeneous catalysts to dendritic,<sup>[3–5]</sup> polymeric organic,<sup>[6]</sup> inorganic or hybrid supports<sup>[7–13]</sup> are some of the examples. Although

such catalysts can be recycled and easily separated from the reaction mixture, they are significantly less active and selective than their homogeneous analogues. Thus, there is increasing urge among the researchers to develop new heterogenised metal complex catalysts capable of recycling several times without appreciable loss of activity.

Mesoporous materials are one of the commonly used solid supports engaged in the heterogenisation of catalysts. The heterogenised catalysts on these solids are used in several chemical transformation, for example, oxidation,<sup>[14]</sup> epoxidation,<sup>[15]</sup> alkane oxidation,<sup>[16]</sup> hydrogenation,<sup>[17]</sup> carbonylation,<sup>[18]</sup> polymerisation,<sup>[19]</sup> C–C coupling reaction<sup>[20,21]</sup> and many others.<sup>[22,23]</sup> A unique advantage of these functionalised mesoporous materials as solid catalyst supports is their high surface areas (>700 m<sup>2</sup> g<sup>-1</sup>) and tunable pore diameters (2–10 nm). To decorate the surface of the mesoporous materials with a suitable metal complex, the complex has to bind strongly at the pore surface in such a way that it fits tightly inside the cavity and does not leach out into the reaction mixture during the catalytic reactions. One of the most challenging areas in this regard is to functionalise the porous support<sup>[24]</sup> in such a way that adequate donor sites are present for a suitable transition metal cation to be heterogenised on its surface, and the resulting material can act as an efficient catalyst. This strategy has been employed in this present work to prepare an immobilised Rh<sup>I</sup> catalyst in which no leaching of metal into the reaction media can take place.

Hydroformylation<sup>[25]</sup> is one of the most important reactions used to convert long-chain alkenes to aldehydes by using carbon monoxide and hydrogen under autogenous pressure. Aldehydes are further utilised to prepare plasti-

[a] Department of Materials Science, Indian Association for the Cultivation of Science, Jadavpur, Kolkata 700032, India  
Fax: +91-33-2473-2805  
E-mail: msab@iacs.res.in

[b] Integrated Science Education and Research Centre (ISERC), Siksha Bhavana, Visva-Bharati University, Santiniketan 731235, India

[c] Department of Chemistry, University of Kalyani, Kalyani, Nadia 741235, India

ciser alcohols and biodegradable detergents, and promote asymmetric intermediates for the synthesis of arylpropionic acids, which are subsequently used in anti-inflammatory drugs, such as ibuprofen or naproxen.<sup>[26,27]</sup> Different metal compounds including Rh,<sup>[28–30]</sup> Ir,<sup>[29,31]</sup> Pt<sup>[32]</sup> and Co<sup>[33]</sup> have been employed as catalysts for such conversions. Different media are also frequently used for such conversions, for example, supercritical carbon dioxide,<sup>[34,35]</sup> ionic liquids<sup>[36,37]</sup> and organic solvents.<sup>[38–40]</sup> Rh<sup>I</sup> complexes have also been used for reductive carbonylation<sup>[41]</sup> and oxidation reactions.<sup>[42]</sup> He et al. have reported a mesoporous silica-anchored Rh–P complex as a catalyst in olefin hydroformylation.<sup>[13,28]</sup> Recently, our group has reported the synthesis of an orthometallated Pd<sup>II</sup> compound anchored onto functionalised mesoporous silica and its efficient use as a heterogeneous catalyst for Suzuki coupling reactions.<sup>[43]</sup>

We herein report the synthesis, characterisation and catalytic application of a rhodium(I)-anchored functionalised mesoporous silica. The material was synthesised by the nitration of the phenyl group anchored onto the silica surface and then reduction to the amine followed by Schiff base condensation. The Schiff base anchored mesoporous matrix is allowed to react with Rh<sup>I</sup> ions to give the covalently grafted Rh<sup>I</sup> catalyst with a large surface area. This com-

pound is used as a heterogeneous catalyst for the hydroformylation reaction of 1-hexene by using a mixture of carbon monoxide and hydrogen at 343 K and 50 bar pressure in *N,N*-dimethylformamide (DMF) as solvent.

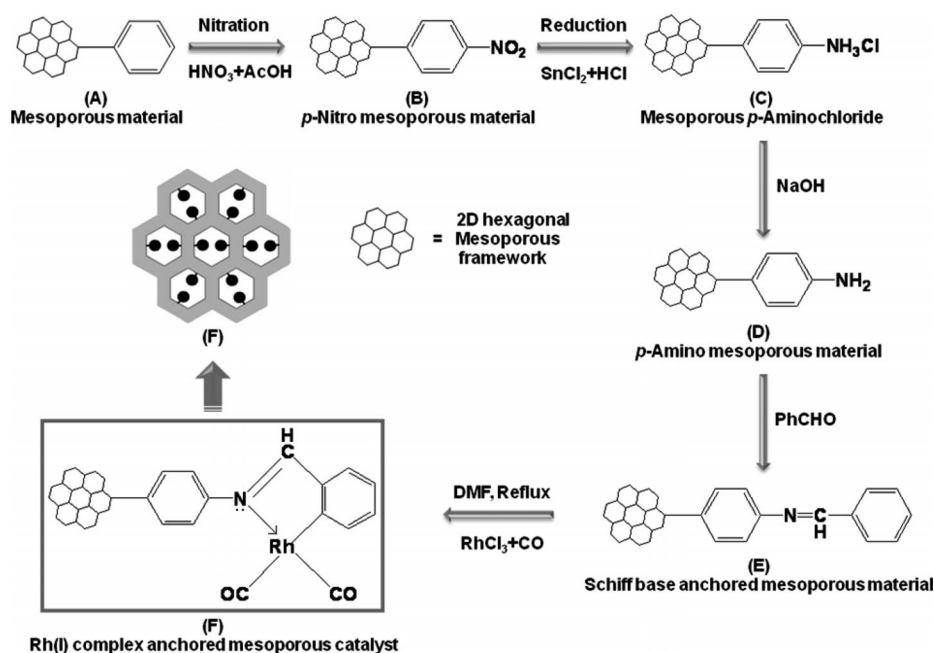
## Results and Discussion

### Differential Elemental Analysis

The results of the elemental analyses of the mesoporous materials **A**, **B**, **D**, **E** and **F** are shown in Table 1. The elemental analysis of the phenyl-functionalised mesoporous material **A** (Scheme 1) showed a carbon content of 16.4% and hydrogen content of 1.5%, which corresponds to approximately 67% phenyl functionalisation if the theoretical molar ratio of the synthesis gel 3:1 for TEOS/PTMOS (TEOS = tetraethyl orthosilicate; PTMOS = phenyltrimethoxysilane) is taken as 100% phenyl functionalisation. This result suggests that the phenyl functionalisation of mesoporous silica occurs almost in a ratio of 5:1 (TEOS/PTMOS), rather than 3:1 used in the synthesis gel. On nitration, 12% of phenyl groups were nitrated, and a further 95% of these nitro groups were converted into the corresponding amine (Table 1). When the amine-functionalised

Table 1. Elemental analyses of mesoporous materials **A**, **B**, **D**, **E** and **F**.

Material	C	H	N	Comment(s)
<b>A</b>	16.4	1.50	–	67% phenyl functionalisation, i.e., considering the theoretical molar ratio of the gel for TEOS/PTMOS (3:1) as 100% phenyl functionalisation
<b>B</b>	16.19	1.59	0.38	12% of ring nitration of the functionalised phenyl group (ref. <sup>[49]</sup> )
<b>D</b>	16.2	2.03	0.38	95% reduction of the converted nitro group to the amine (ref. <sup>[49]</sup> )
<b>E</b>	18.11	1.68	0.38	90% amine group underwent Schiff base functionalisation
<b>F</b>	17.91	1.65	0.37	47% of Schiff base donor sites coordinate with Rh <sup>I</sup> based on 1.04 wt.-% loading of Rh in mesoporous catalyst as obtained from independent AAS analysis



Scheme 1. Functionalisation of the mesoporous organosilica surface with Rh<sup>I</sup>.

material **D** was allowed to react with benzaldehyde, 90% of the amine groups undergo Schiff base condensation to produce **E**. These three observations are corroborated by the elemental analysis results in Table 1. The carbon, hydrogen and nitrogen contents of sample **F** (Scheme 1) containing the Schiff base functionalised Rh complex are 17.91, 1.65 and 0.37 wt.-%, respectively. The amount of Rh in **F** has been found to be 1.04 wt.-% from chemical analysis by using atomic absorption spectroscopy (AAS). This Rh loading amount suggested that about 47% of the Schiff base donor sites in **F** are coordinated by Rh, and these sites are responsible for the hydroformylation reaction.

### Characterisation of the Catalyst

The low-angle powder X-ray diffraction patterns of the as-synthesised and extracted samples (Figure 1a and b, respectively) show four intense peaks, which correspond to the presence of a 2D-hexagonal mesophase in the samples. The Schiff base ligand anchored mesoporous material **E** (Figure 1c) also showed one intense and two weaker peaks in the low-angle region, which indicate that the ordered structure is retained after organic modification. For the Rh-loaded sample **F** (Figure 1d), however, only one intense peak corresponding to the 100 plane of the mesophase was obtained in the low-angle region, suggesting that the rigorous process of Rh loading decreases the ordering in the sample to some extent. The diffraction pattern of sample **F** after two catalytic cycles (Figure 1e) also retained the peak corresponding to the 100 plane of the mesophase, but the peak shifted to a smaller  $d$  value, suggesting a little shrinkage in the pore size. The wide-angle XRD pattern of this sample is devoid of any peak indicating the absence of metallic Rh in the material. The high-resolution TEM image of the as-synthesised silica sample shown in Figure 2a reveals a highly ordered hexagonal arrangement of the pores, which is again confirmed by the selected area electron diffraction (SAED) pattern shown in the inset. The TEM image of the Rh-loaded sample **F** (Figure 2b), on the other hand, only exhibits a hexagonally ordered mesostructure in some parts of the specimen. Thus, the powder XRD pattern and TEM image analysis suggest that the Rh-loaded sample partially retains its hexagonal ordering of the pores.

$N_2$  adsorption/desorption isotherms of the extracted mesoporous phenyl silica material **A**, the Rh-loaded material **F** and the Rh-loaded material **F** after two catalytic cycles, are shown in Figure 3a–c, respectively. The samples followed a typical type IV isotherm, characteristic of the mesopores.<sup>[45]</sup> The BET surface area of the extracted sample **A** was found to be  $827 \text{ m}^2 \text{ g}^{-1}$ , the Rh-loaded sample had a surface area of  $685 \text{ m}^2 \text{ g}^{-1}$ , and the surface area of the Rh-loaded sample after two catalytic cycles was  $530 \text{ m}^2 \text{ g}^{-1}$ . After the loading of the Rh<sup>I</sup> complex, a substantial decrease in surface area and pore volume takes place, which implies that the complex is bound mostly within the inner surface of the pores. After two catalytic cycles, there is some shrinkage in the pore structure, which is reflected in the lower

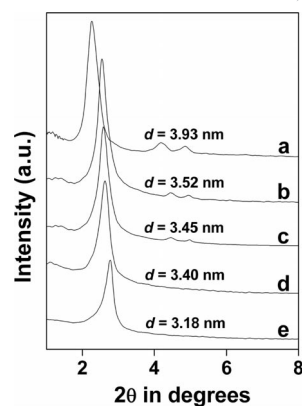


Figure 1. Low-angle PXRD pattern of (a) the as-synthesised sample, (b) the extracted sample **A**, (c) Schiff base ligand anchored mesoporous material **E**, (d) Rh-loaded sample **F**, (e) Rh-loaded sample **F** after two catalytic cycles;  $d_{100}$  spacing for different samples is shown along with the respective curves.

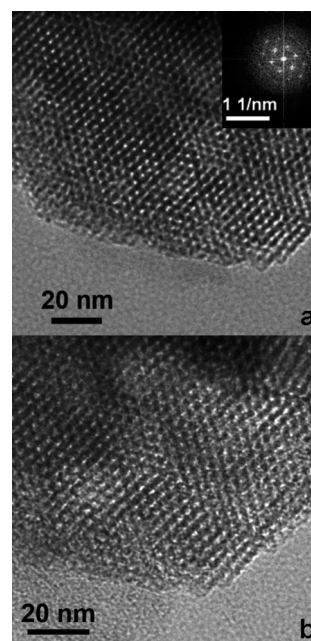


Figure 2. TEM images of (a) the phenyl-functionalised mesoporous silica with selected-area electron-diffraction pattern shown in the inset, (b) Rh<sup>I</sup>-loaded material **F**.

surface area of the used catalyst. In the inset of Figure 3, the pore size distributions (PSD) of the samples (a'–c') estimated by using the non-local density functional theory (NLDFT)<sup>[46]</sup> method are shown. The PSD patterns are quite narrow, which indicates the presence of uniform mesopores of similar dimensions throughout the bulk of the sample. A bimodal kind of distribution of pores was obtained with peak pore diameters at 2 and 5.5 nm for sample **A**, and 1.65 and 4.9 nm for sample **F**. These data are in good agreement with the TEM image analysis. The origin of large mesopores for both the samples (5.5 and 4.9 nm, respectively) may be attributed to the presence of H<sub>2</sub>-type nonparallel adsorption and desorption branches of the  $N_2$  sorption isotherms.<sup>[47]</sup> These could originate from the cages

generated for the phenyl group/Rh complex partially present at the outer surface of the material. Broadening of the peak in the PSD for the used catalyst (Figure 3c') suggested a decrease in the mesoscale periodicity after two repetitive catalytic cycles. Pore volumes estimated from the adsorption isotherms for samples A and F were 0.49 and 0.44 cc g<sup>-1</sup>, respectively. Thus, the pore volume for the Rh-loaded mesoporous material is sufficient to carry out the hydroformylation reaction of 1-hexene. Although the pore volume of the used catalyst after two repeat cycles decreased to 0.246 cc g<sup>-1</sup>, the catalytic activity of the same after further reactions remained high (see below; Scheme 2).

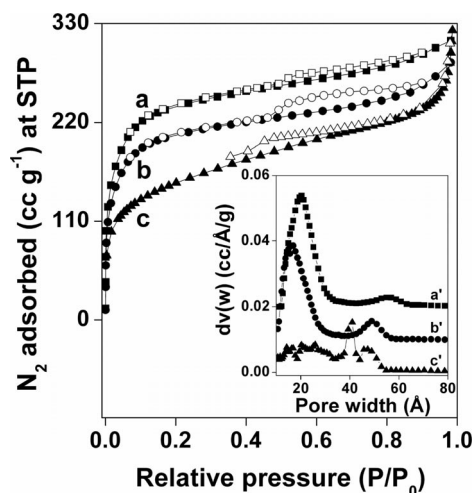
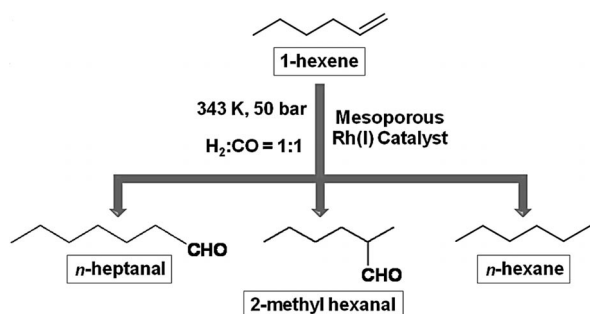


Figure 3. Nitrogen adsorption/desorption isotherms of (a) extracted sample A, (b) Rh<sup>I</sup>-loaded material F, and (c) Rh<sup>I</sup>-loaded material F after two catalytic cycles. Inset: Pore-size distribution of (a') A, (b') F and (c') F after two catalytic cycles. Plots a' and b' are offset by 0.02 and 0.01 cm<sup>3</sup> Å<sup>-1</sup> g<sup>-1</sup>, respectively.



Scheme 2. Reaction pathways for the hydroformylation of 1-hexene.

The FTIR spectra of the different materials obtained after various stages of reaction are shown in Figure 4. The spectrum of material A (Figure 4a) shows a  $\nu_{C-H}$  band in the region of 3100–2800 cm<sup>-1</sup>, ca. 1600, ca. 1500 and 1460 cm<sup>-1</sup> for skeletal vibrations and 760 and 680 cm<sup>-1</sup> for C–H bending. For the nitrated material B (Figure 4b), the appearance of two strong new IR peaks at 1530 and 1354 cm<sup>-1</sup> with another new peak at 835 cm<sup>-1</sup> is evidence of the nitro group introduced in the *para* position of the phenyl group of A.<sup>[6]</sup> The intensities of FTIR peaks for  $\nu_{NO_2}$  in material C (not shown) are reduced with the ap-

pearance of a new peak at 2550 cm<sup>-1</sup>. Material D exhibits strong multiple bands in the region 3400–3200 cm<sup>-1</sup> ( $\nu_{NH_2}$ ) and a shoulder at 1625 cm<sup>-1</sup> ( $\delta_{NH_2}$ ) with the disappearance of the peak at 2550 cm<sup>-1</sup>. For material E (Figure 4d) the peak at 1653 cm<sup>-1</sup> may be assigned to the formation of >C=N, which is evidence of the Schiff base condensation between the benzaldehyde and the functionalised amine. The Rh catalyst F exhibits a peak at 1644 cm<sup>-1</sup> (Figure 4e) confirming the coordination of the >C=N bond to the metal atom. Two new peaks at 1982 and 2083 cm<sup>-1</sup> reveal the presence of a CO group in the catalyst, and the peak at 722 cm<sup>-1</sup> depicts the *ortho*-metallation of the phenyl ring with Rh<sup>I</sup>.<sup>[44]</sup> The FTIR spectra of F after two catalytic cycles (Figure 4f) is similar to the fresh material F, which points to the fact that after reaction there is no change in the composition of the catalyst.

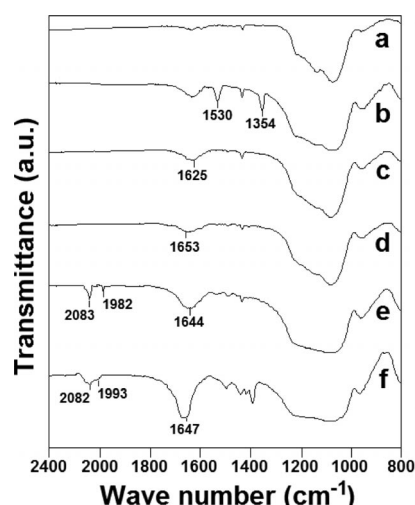


Figure 4. FTIR spectra of (a) extracted sample A, (b) *p*-nitro-functionalised mesoporous material B, (c) *p*-amino mesoporous material D, (d) Schiff base ligand anchored mesoporous material E, (e) Rh-loaded sample F, and (f) Rh-loaded sample F after two catalytic cycles.

### Catalytic Activity

The Rh<sup>I</sup>-containing mesoporous material F has been examined for its catalytic efficiency in the hydroformylation reaction of 1-hexene to *n*-heptanal. The reaction product consisted of a mixture of branched and linear aldehydes. The reaction conditions were optimised by varying the reaction parameters, and the results are summarised in Table 2. We first investigated the effect of the temperature on 1-hexene hydroformylation reactions. The temperature had a considerable effect, not only on the reaction rate but also on the selectivity of the main and side reactions. As the temperature increased from 313 to 353 K, the conversion of 1-hexene increased, and at 353 K the highest conversion was obtained. At first, the yield of aldehydes increased and then decreased with increasing temperature. The selectivity of *n*-heptanal reached the highest value of 78% when the temperature was increased to 343 K. As the temperature

Table 2. Effect of reaction parameters on the hydroformylation reaction of 1-hexene.<sup>[a]</sup>

Entry	Temperature [K]	Pressure [bar]	H <sub>2</sub> /CO ratio	Conversion [%]	Selectivity [%]		
					<i>n</i> -Heptanal	2-Methylhexanal	Hexane
1.	313	50	1:1	12	48	29	23
2.	323	50	1:1	25	55	26	19
3.	333	50	1:1	56	70	22	8
4.	343	50	1:1	72	78	18	4
5.	353	50	1:1	74	69	15	16
6.	343	40	1:1	59	76	14	10
7.	343	60	1:1	72	78	18	4
8.	343	50	0.5:1	34	53	21	26
9.	343	50	1.5:1	65	70	21	9

[a] Catalyst: Rh<sup>I</sup>-containing functionalised 2D-hexagonal mesoporous material (0.02 g); solvent: DMF.

was further increased, selectivity began to decrease. At higher temperature, the hydrogenated product predominated and hence the optimal temperature was adopted at 343 K. The effect of pressure and H<sub>2</sub>/CO ratio on the hydroformylation reaction was also investigated. As shown in Table 2, a total pressure of 50 bar with an H<sub>2</sub>/CO ratio of 1:1 leads to the best conversion (Entry 4) of 1-hexene. The conversion increased from 34 to 72% when the H<sub>2</sub>/CO ratio was increased from 0.5:1 to 1:1. A higher H<sub>2</sub>/CO ratio (1.5:1) did not improve the conversion. The major products obtained during the reaction were *n*-heptanal and 2-methylhexanal along with that a small amount of hydrogenated product, i.e. *n*-hexane, was also produced.

### Heterogeneity Tests

To determine whether the catalyst actually functions in a heterogeneous manner, a hot-filtration test was performed on the hydroformylation reaction of 1-hexene. During the catalytic hydroformylation reaction of 1-hexene, the solid catalyst was separated from the reaction mixture by filtration after 4 h. The conversion of 1-hexene at this point was 38.0%. In Figure 5 we compare the concentration profiles of 1-hexene in the hot-filtration experiment with a normal catalytic experiment (uninterrupted) using the same Rh-loaded functionalised mesoporous catalyst in which the reaction was carried out for a further 4 h. The gas chromatographic analysis showed no increase in the conversion in the hot-filtration test (Figure 5b), whereas there is an increase in conversion in the uninterrupted experiment (Figure 5c). AAS analyses of the liquid phase of the reaction mixtures collected by filtration confirmed that Rh is absent in the reaction mixture. These results suggest that the Rh is not being leached out from the catalyst during the hydroformylation reactions. Furthermore, when the reaction was carried out in the absence of catalyst (blank reaction), no hydroformylation of 1-hexene was observed (Figure 5a). This result suggested the catalytic role played by the Rh<sup>I</sup> centre in this hydroformylation reaction.

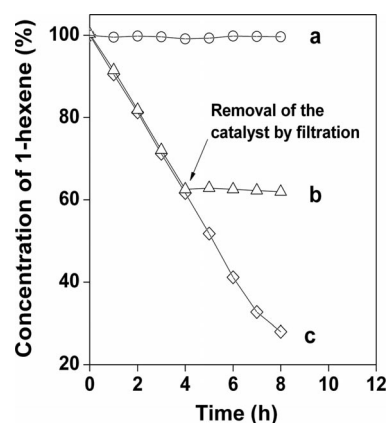


Figure 5. Concentration profiles of 1-hexene: (a) blank experiment without catalyst, (b) normal experiment in the presence of Rh catalyst, (c) hot-filtration test; reaction temperature 343 K, H<sub>2</sub>/CO = 1:1.

### Catalyst Recycling

One of the main advantages of a heterogeneous catalyst is to enhance the lifetime of the catalyst. To investigate the reusability of the mesoporous Rh<sup>I</sup> complex, the catalyst was separated by filtration after the first run, dried under vacuum and then subjected to a second run under the same reaction conditions. The catalytic reaction was repeated

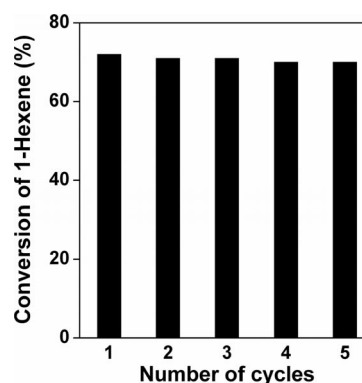


Figure 6. Recycling efficiency for the hydroformylation of 1-hexene in the presence of Rh<sup>I</sup>-anchored mesoporous silica.

with further addition of substrates in the appropriate amount under optimum reaction conditions, and the nature and yield of the final products were found to be comparable to that of the original one. As seen in Figure 6, the catalyst can be reused up to five times without any appreciable loss of its catalytic activity. An AAS study has been used to determine the amount of Rh leached into the DMF solution during the reaction, and it was found that there was almost no Rh leaching into the liquid phase from the immobilised catalyst.

## Conclusion

We have described the synthesis of a phenyl-functionalised 2D-hexagonal mesoporous silica material through a mixed surfactant templating route, followed by the functionalisation of the phenyl group for anchoring an *ortho*-metallated Rh<sup>I</sup> complex. The supported Rh<sup>I</sup> complex acts as an efficient catalyst in the hydroformylation reaction of 1-hexene and exhibits high selectivity for the one-carbon-elongated *n*-heptanal. Good catalytic activity and efficiency in this one-carbon addition reaction suggest the potential application of this functionalised mesoporous material in the synthesis of value-added organic target molecules. We believe that our synthetic strategy for anchoring the Rh complex to the surface of the mesoporous material and its successful use as heterogeneous catalyst in the hydroformylation reactions would motivate researchers to design relevant active heterogeneous catalysts having a suitably anchored metal complex as catalytic centres, which may open up new catalytic applications.

## Experimental Section

**General:** The mesoporous organosilica was prepared by minor modifications to the procedure described previously.<sup>[43]</sup> In a typical synthesis, cetylpyridinium chloride (CPC; Loba Chemie; 3.58 g,  $1 \times 10^{-2}$  mol) and Brij-35 [C<sub>12</sub>H<sub>25</sub>(OC<sub>2</sub>H<sub>4</sub>)<sub>23</sub>OH; Loba Chemie; 1.2 g] were dissolved in an acidic aqueous solution of tartaric acid (TA; E. Merck; 0.6 g of TA in 70 g of H<sub>2</sub>O) under vigorous stirring at room temp. for 1 h. A mixture of tetraethyl orthosilicate (TEOS; Sigma–Aldrich; 6.25 g,  $3.0 \times 10^{-2}$  mol) and phenyltrimethoxysilane (PTMOS; Sigma–Aldrich; 1.99 g,  $1.0 \times 10^{-2}$  mol) were added to the mixture under continuous stirring for 0.5 h. Tetramethylammonium hydroxide (TMAOH; Sigma–Aldrich, 25% aqueous solution) was then added dropwise, and the solution was maintained at pH  $\approx 10.5$ . The resulting mixture was stirred at 298 K for 24 h and then treated hydrothermally at 348 K for 72 h followed by filtration, drying and extraction with acidic ethanol to yield the phenyl-functionalised mesoporous silica **A**. Analytical-grade reagents and freshly distilled solvents, pure and dry hydrogen gas and pre-distilled solvents were used throughout the investigation. Liquid substrates were pre-distilled and dried by appropriate molecular sieves, and solid substrates were recrystallised before use. Chemical analysis was done according to a literature procedure.<sup>[48]</sup> The purities of solvents and substrates were checked by GC.

**Preparation of *p*-Nitro Mesoporous Material (B):** The *p*-nitro-functionalised mesoporous material **B** was prepared according to the method of King and Sweet.<sup>[49]</sup> A suspension of the mesoporous

material (5 g) was constantly stirred in a mixture of acetic anhydride (20 mL), nitric acid (70%, 2 mL) and glacial acetic acid (4 mL) at 278 K for 30 min and then at 373 K for 24 h. The obtained *p*-nitro mesoporous material was washed successively with acetic acid, THF, water and methanol, and finally dried under vacuum in a lypholyzer.

**Preparation of *p*-Amino Mesoporous Material (D):** A mixture of acetic acid (20 mL), stannous chloride (5 g), concentrated hydrochloric acid (6 mL) and *p*-nitro mesoporous material (5 g) was stirred at 373 K for 72 h to reduce the nitro compound to the corresponding amine hydrochloride **C**.<sup>[6]</sup> The residue, after filtration, was washed several times with methanol and then successively with THF. Compound **C**, on repeated treatment with sodium bicarbonate solution (0.01 M), produced the corresponding free amine **D**. This was washed with methanol and dried under vacuum in a lypholyzer.

**Preparation of the Schiff Base Anchored Mesoporous Material (*p*-C<sub>6</sub>H<sub>4</sub>N=CHPh, E) and the Corresponding Rh<sup>I</sup> Mesoporous Material (F):** A suspension of the *p*-amino mesoporous material (3 g) in dry toluene (30 mL) containing an excess of the carbonyl compound C<sub>6</sub>H<sub>5</sub>CHO was refluxed at 403 K under dry nitrogen for 72 h by using a Dean–Stark apparatus.<sup>[6]</sup> The resulting material was filtered, washed successively with benzene, THF and ethanol, and then dried under vacuum in a lypholyzer. The Rh<sup>I</sup> complex was prepared according to a published procedure with a slight modification.<sup>[50]</sup> CO gas was continuously bubbled through a deep-red mixture of RhCl<sub>3</sub>·3H<sub>2</sub>O (Sigma–Aldrich; 0.2 g) and the Schiff base ligand anchored mesoporous silica **E** (1.0 g) in dry, deoxygenated DMF (10 mL) and refluxed for 12 h. The resulting material was filtered, washed successively with DMF, THF and ethanol, and then dried under vacuum in a lypholyzer. A flow diagram for the preparation of the Rh-anchored mesoporous material **F** is shown in Scheme 1. The loading of Rh onto **F**, estimated by AAS, was 1.04 wt.-%. Powder X-ray diffraction patterns of the materials were recorded with a Bruker D8 Advance diffractometer operated at 40 kV and 40 mA and calibrated with a standard silicon sample by using Ni-filtered Cu-K<sub>α</sub> ( $\lambda = 0.15406$  nm) radiation. TEM images were recorded with a Jeol JEM 2010 TEM operated at an accelerated voltage of 200 kV. Nitrogen adsorption/desorption isotherms were obtained by using an Autosorb 1C at 77 K. Prior to gas adsorption measurements, the samples were degassed at 423 K for 4 h. FTIR spectra of the samples were recorded on KBr pellets with a Nicolet MAGNA-FT IR 750 spectrometer series II. AAS studies were carried out with a Shimadzu AA-6300 atomic absorption spectrophotometer. The reaction products were analyzed with a Varian 3400 gas chromatograph equipped with a 30 m CP-SIL8CB capillary column and a flame ionisation detector. All reaction products were identified with an Agilent GC–MS (QP-5050) gas chromatograph.

**Reaction Procedure for Catalytic Hydroformylation Reaction of 1-Hexene:** The hydroformylation reaction of 1-hexene was carried out in a 100 mL stainless steel autoclave reactor with inlet and outlet that was equipped with a Teflon liner containing a stirring bar. The mesoporous Rh<sup>I</sup> catalyst (0.02 g), 1-hexene (0.063 g, 0.75 mmol) and dried DMF (10 mL) were placed into the autoclave. The autoclave was flushed three times with CO gas and pressurised to 25 bar; H<sub>2</sub> gas was then introduced up to a total pressure of 50 bar. The reactor was then heated at 343 K for 8 h. After completion of the reaction, the autoclave was cooled to room temp., the excess CO/H<sub>2</sub> was released, and the catalyst was separated from the reaction mixture by filtration.

## Acknowledgments

A. B. and M. I. wish to thank the Department of Science & Technology, New Delhi for financial support. This work was partly funded by the Nanoscience and Nanotechnology Initiative of the Department of Science & Technology.

- [1] P. Anastas, J. Warner, *Green Chemistry: Theory and Practice*, Oxford University Press, USA, **1998**.
- [2] *Applied Homogeneous Catalysis with Organometallic Compounds* (Eds.: B. Cornils, W. A. Herrmann), VCH, Weinheim, **1996**.
- [3] R. Kreiter, A. W. Kleij, R. J. M. Klein Gebbink, G. van Koten, in *Dendrimers IV: Metal Coordination, Self-Assembly, Catalysis* (Eds.: F. Vögtle, C. A. Schalley), Springer-Verlag, Berlin, **2001**, vol. 217, p. 163.
- [4] R. van Heerbeek, P. C. J. Kamer, P. W. N. M. van Leeuwen, J. N. H. Reek, *Chem. Rev.* **2002**, *102*, 3717–3756.
- [5] G. E. Oosterom, J. N. H. Reek, P. C. J. Kamer, P. W. N. M. van Leeuwen, *Angew. Chem. Int. Ed.* **2001**, *40*, 1828–1849.
- [6] S. M. Islam, A. Bose, B. K. Palit, C. R. Saha, *J. Catal.* **1998**, *173*, 268–281.
- [7] C. E. Song, S.-G. Lee, *Chem. Rev.* **2002**, *102*, 3495–3524.
- [8] Y. R. de Miguel, E. Brulé, R. G. Margue, *J. Chem. Soc. Perkin Trans. 1* **2001**, 3085–3094.
- [9] C. González-Arellano, A. Corma, M. Iglesias, F. Sánchez, *Eur. J. Inorg. Chem.* **2008**, 1107–1115.
- [10] S. Bräse, F. Lauterwasser, R. E. Ziegert, *Adv. Synth. Catal.* **2003**, *345*, 869–929.
- [11] A. D. Zotto, C. Greco, W. Baratta, K. Siega, P. Rigo, *Eur. J. Inorg. Chem.* **2007**, 2909–2916.
- [12] S. Mukherjee, S. Samanta, B. C. Roy, A. Bhaumik, *Appl. Catal. A* **2006**, *301*, 79–88.
- [13] W. Zhou, D. H. He, *Chem. Commun.* **2008**, 5839–5841.
- [14] a) V. Ayala, A. Corma, M. Iglesias, F. Sánchez, *J. Mol. Catal. A* **2004**, *221*, 201–208; b) A. Castro, J. C. Alonso, A. A. Valente, P. Neves, P. Brandao, V. Felix, P. Ferreira, *Eur. J. Inorg. Chem.* **2010**, *9*, 1405–1412.
- [15] a) J. Chakraborty, M. Nandi, H. Mayer-Figge, W. S. Sheldrick, L. Sorace, A. Bhaumik, P. Banerjee, *Eur. J. Inorg. Chem.* **2007**, 5033–5044; b) P. Roy, M. Nandi, M. Manassero, M. Mazzani, M. Riccò, A. Bhaumik, P. Banerjee, *Dalton Trans.* **2009**, 9543–9554.
- [16] V. N. Shetti, M. J. Rani, D. Srinivas, P. Ratnasamy, *J. Phys. Chem. B* **2006**, *110*, 677–679.
- [17] a) H. Li, H. Lin, S. Xie, W. Dai, M. Qiao, Y. Lu, H. Li, *Chem. Mater.* **2008**, *20*, 3936–3943; b) C. González-Arellano, A. Corma, M. Iglesias, F. Sánchez, *Catal. Today* **2005**, *107–108*, 362–370; c) V. Ayala, A. Corma, M. Iglesias, J. A. Rincón, F. Sánchez, *J. Catal.* **2004**, *224*, 170–177.
- [18] K. Mukhopadhyay, B. R. Sarkar, R. V. Chaudhari, *J. Am. Chem. Soc.* **2002**, *124*, 9692–9693.
- [19] P. W. Kletnieks, A. J. Liang, R. Craciun, J. O. Ehresmann, D. M. Marcus, V. A. Bhirud, M. M. Klaric, M. J. Hayman, D. R. Guenther, O. P. Bagatchenko, D. A. Dixon, B. C. Gates, J. F. Haw, *Chem. Eur. J.* **2007**, *13*, 7294–7304.
- [20] a) J. Demel, M. Lamac, J. Cejka, P. Stepnicka, *ChemSusChem* **2009**, *2*, 442–451; b) Y. Wan, H. Wang, Q. Zhao, M. Klingstedt, O. Terasaki, D. Zhao, *J. Am. Chem. Soc.* **2009**, *131*, 4541–4550.
- [21] a) C. González-Arellano, A. Corma, M. Iglesias, F. Sánchez, *Adv. Synth. Catal.* **2004**, *346*, 1758–1764; b) A. Corma, C. González-Arellano, M. Iglesias, S. Pérez-Ferreras, F. Sánchez, *Synlett* **2007**, *11*, 1771–1774.
- [22] Z. Wang, G. Chen, K. Ding, *Chem. Rev.* **2009**, *109*, 322–359.
- [23] R. N. Shiju, V. V. Gulians, *Appl. Catal. A: Gen.* **2009**, *356*, 1–17.
- [24] D. Chandra, A. Dutta, A. Bhaumik, *Eur. J. Inorg. Chem.* **2009**, 4062–4068.
- [25] F. Ungváry, *Coord. Chem. Rev.* **2007**, *251*, 2072–2086.
- [26] A. M. Trezeciak, J. J. Ziolkowski, *Coord. Chem. Rev.* **1999**, *190–192*, 883–900.
- [27] *Rhodium Catalyzed Hydroformylation* (Eds.: P. W. N. M. van Leeuwen, C. Claver), Kluwer Academic Publishers, Dordrecht, **2000**.
- [28] W. Zhou, D. H. He, *Green Chem.* **2009**, *11*, 1146–1154.
- [29] X.-Y. Yi, K.-W. Chan, E. K. Huang, Y.-K. Sau, I. D. Williams, W.-H. Leung, *Eur. J. Inorg. Chem.* **2010**, 2369–2375.
- [30] K. Mukhopadhyay, A. B. Mandale, R. V. Chaudhari, *Chem. Mater.* **2003**, *15*, 1766–1777.
- [31] M. A. Moreno, M. Haukka, T. A. Pakkanen, *J. Catal.* **2003**, *215*, 326–331.
- [32] G. Petöcz, G. Rangits, M. Shaw, H. de Bod, D. B. G. Williams, L. Kollár, *J. Organomet. Chem.* **2009**, *694*, 219–222.
- [33] M. J. Chen, R. J. Klingler, J. W. Rathke, K. W. Kramarz, *Organometallics* **2004**, *23*, 2701–2707.
- [34] I. Kani, R. Flores, J. P. Fackler Jr., A. Akgerman, *J. Supercrit. Fluids* **2004**, *31*, 287–294.
- [35] D. Koch, W. Leitner, *J. Am. Chem. Soc.* **1998**, *120*, 13398–13404.
- [36] P. B. Webb, T. E. Kunene, D. J. Cole-Hamilton, *Green Chem.* **2005**, *7*, 373–379.
- [37] C. P. Mehnert, R. A. Cook, N. C. Dispenziere, M. Afeworki, *J. Am. Chem. Soc.* **2002**, *124*, 12932–12933.
- [38] F. Favre, H. Olivier-Bourbigou, D. Commereuc, L. Saussine, *Chem. Commun.* **2001**, 1360–1361.
- [39] D. A. Aubry, N. N. Bridges, K. Ezell, G. G. Stanley, *J. Am. Chem. Soc.* **2003**, *125*, 11180–11181.
- [40] O. Hemminger, A. Marteel, M. R. Mason, J. A. Davies, A. R. Tadd, M. A. Abraham, *Green Chem.* **2002**, *4*, 507–512.
- [41] S. M. Islam, D. Mal, B. K. Palit, C. R. Saha, *J. Mol. Catal. A* **1999**, *142*, 169–181.
- [42] P. M. Reddy, A. V. S. S. Prasad, C. K. Reddy, V. Ravinder, *Transition Met. Chem.* **2008**, *33*, 251–258.
- [43] K. Sarkar, M. Nandi, M. Islam, M. Mubarak, A. Bhaumik, *Appl. Catal. A* **2009**, *352*, 81–86.
- [44] J. M. Esparza, M. L. Ojeda, A. Campero, G. Hernández, C. Felipe, M. Asomoza, S. Cordero, I. Kornhauser, F. Rojas, *J. Mol. Catal. A* **2005**, *228*, 97–110.
- [45] D. Chandra, S. C. Laha, A. Bhaumik, *Appl. Catal. A: Gen.* **2008**, *342*, 29–34.
- [46] P. I. Ravikovitch, A. V. Neimark, *J. Phys. Chem. B* **2001**, *105*, 6817–6823.
- [47] K. Sarkar, T. Yokoi, T. Tatsumi, A. Bhaumik, *Microporous Mesoporous Mater.* **2008**, *110*, 405–412.
- [48] *Vogel's Textbook of Quantitative Analysis* (Eds.: J. Mendham, R. C. Denney, J. D. Barnes, M. J. K. Thomas), 6th ed., Pearson Education Ltd., New Delhi, **2007**, 495.
- [49] R. B. King, E. M. Sweet, *J. Org. Chem.* **1979**, *44*, 385–391.
- [50] K. Hiraki, Y. Obayashi, Y. Oki, *Bull. Chem. Soc. Jpn.* **1979**, *52*, 1372–1376.

Received: August 6, 2010

Published Online: December 2, 2010